J. Rubb. Res., **14(3)**, 139–150

Synthesis and Photocatalytic Activity of Natural Rubber/Titanates Nanocomposite

K.S. TAN*# AND J. RILEY**

One dimensional (1-D) sodium titanate nanoparticles have been synthesised using a hydrothermal reaction. The photocatalytic properties of natural rubber (NR) based nanocomposite containing sodium titanate are presented. Rhodamine B (RhB) was used as the target organic material for photocatalysis studies. The degradation of RhB molecules was monitored using a fluoremeter, based on the fluorescent emission counts of RhB sample solution subjected to ultraviolet (UV) light irradiation. The nanocomposite was photocatalytically active and the RhB degradation efficiency largely depends on the crystal phase of titanates and the distribution of photocatalysts on the NR surface.

Keywords: photocatalysis; sodium titanate; rhodamine B; crystal structure; fluorescent; natural rubber; nanocomposite; UV degradation

Many applications of photoactive titanates are developed based on photocatalysis. Among the applications, bactericide[1–4] can be considered as commercially viable. One of the original applications of photocatalysis was in the field of energy conversion but since the conversion efficiency was low, attention has been shifted to the strong oxidative property of photocatalysts. To study the antibacterial ability of photocatalysts, simple organic molecules can be used instead of actual bacteria; including rhodamine B[5–10,11], congo red[12], alcohol[13] and carbon dioxide[14]. In this paper, photocatalysis investigations were carried out using rhodamine B as target molecules. The breakdown of RhB molecules under UV light in the presence of titanium oxides as catalysts has been widely studied[5,10,15–18]. Most of the research work using RhB as target molecules employs UV-vis spectroscopy to monitor the degradation rate[5,7,11,19]. In our work, a fluoremeter instead of UV-vis was used to monitor the concentration of RhB in aqueous solution. A solution of fluorescently active rhodamine B molecules in the presence of a titanate was subjected to UV light and the rhodamine B fluorescence was monitored as a function of irradiation time.

Various supporting materials have been used to immobilise photo active particles. This approach affects some of the photocatalytic capability of the material, but it is a compromise between easy handling and effectiveness[20]. Activated carbon and silicon rubber have been employed to enhance the adsorption of organic matter, as reported by Gao[21]. Immobilisation of photoactive nanoparticles

*Rubber Research Institute of Malaysia, Malaysian Rubber Board, P.O. Box 10150, 50908 Kuala Lumpur, Malaysia.
** Department of Materials, Imperial College London, Exhibition Road, London, SW7 2AZ, United Kingdom.
# Corresponding author (e-mail: kstan@lgm.gov.my)

can also be carried out using electrophoretic deposition as described by Nawi[22]. There are reports that show the photocatalytic reactivity of titanium oxide actually increases through immobilisation on Zeolite particles[14]. We report the use of NR as a supporting material to the titanate nanoparticles.

EXPERIMENTAL

Materials

Natural rubber (NR) latex was obtained from the Malaysian Rubber Board (MRB). The latex had been pre-vulcanised (PV) with some chemical compounds and processes. *Table 1* shows the formulation used in making the PV latex which was prevulcanised at 60ºC for 5 hours. The quantities shown in the table are based on parts per hundred rubber (p.h.r.) which is a widely used standard in the NR industry.

TABLE 1. FORMULATION OF PV LATEX USED IN THE STUDY

Latex composition	Quantity, p.h.r.
60% high ammonia latex	100
10% non-ionic surfactant	0.1
70% t-butyl hydroperoxide (tBHP)	0.9
10% tetraethylene pentamine	0.8

One dimensional (1-D) titanate nanoparticles were synthesised *via* hydrothermal reaction using anatase nanopowder purchased from Sigma-Aldrich without further purification. Milipore water with resistivity greater than 18MΩ was used in the dissolution and all washing works. The PTFE-lined autoclave set up was bought from the PARR Instrument Company, Moline. Illinois. U.S.A.

Preparation of Stock Solution

0.0253 g of rhodamine was dissolved in 17.1648 g of water in a glass vial and well mixed using an ultrasound bath. 0.5 mL of the solution was transferred into a 1L standard flask and topped up with deionised water. The final concentration of stock solution was 1.538×10^{-6} mol dm^{-3}. The flask was wrapped with aluminium foil to avoid any contact with background UV light.

Preparation of 1-D Titanates

In a typical preparation, an accurate amount of anatase powder was weighed and transferred into a PTFE container. A desired amount of 10 mol dm^{-3} NaOH solution was added with a pipette to obtain a concentration of 0.008 g cm^{-3}. The solution was mixed thoroughly using a magnetic stirrer. Without removing the magnetic bar, the PTFE container was sealed, using PTFE tape around the container lid, which was also made of PTFE. The container was inserted into a stainless steel vessel with the stainless steel lid screwed on tightly before heating in a preheated oven at 180ºC. After the desired reaction time was reached, the container was removed from the oven and was allowed to cool down to room temperature. The resultant slurry in the PTFE container was removed and filtered using Whatman qualitative filter paper and washed thoroughly with water. The sludge was transferred into a glass container and water was added to make a dispersion. HCl was added to the dispersion until the pH was 2. The dispersion was left stirring magnetically over night to allow ion exchange between Na^+ and H^+. After that, the dispersion was filtered and fresh water was added into the slurry and the final pH was adjusted to pH 7 using HCl and NH_4OH. The resultant dispersion was filtered again and the sample was dried in an oven at 60ºC overnight. The nanotubes were similarly obtained except

that 0.08 g cm^{-3} of anatase and 7.5 mol dm^{-3} of NaOH were used.

Preparation of NR/Titanate Nanocomposites

0.12 g sodium titanate was suspended in 4.5 mL of water and 1.0 mL of this suspension was added into a vial containing 0.25 mL of 60% PV latex. 0.1 mL of this mixture was transferred onto a pre-cast NR strip by a pipette and levelled out using the tip of the pipette itself. The dimension of the NR strip was 8 mm × 40 mm × 1 mm. A total of 0.0035 g of dried sample was loaded onto each NR strip. This is an equivalent of 1 p.h.r., based on the total weight of the nanocomposites. The coating was dried in an oven at 60ºC for 30 min. The composite strip was then inserted into a quartz cuvette, as shown in *Figure 1*. The dimension of the strip was designed to fit the side wall so that the strip could remain immobilised throughout the test. This is important because NR has a density of 0.96 g cm^{-3} and will float on the test solution if it was not held in place. The titanate coated surface was facing the UV source and in contact with the rhodamine B solution. Two nanocomposite strips were fabricated; one with nanorods and the other with nanotubes; both used the same weight of material. The photocatalytic activity of the nanocomposites was compared.

Set Up

Since most of the plastic and glass materials absorb UV light, the set up of this experiment needs more consideration. Quartz is an ideal material that is transparent to UV light. Some researchers have used petri dishes[28] and arranged the UV lamp right on top of the dish to avoid the UV light being absorbed by the container. This set up is simple and inexpensive. However, the open exposure of sample solution to the air means a faster rate of evaporation. For a small sized sample, the loss of water volume can affect the accuracy of the results obtained. The set up (*Figure 1*)

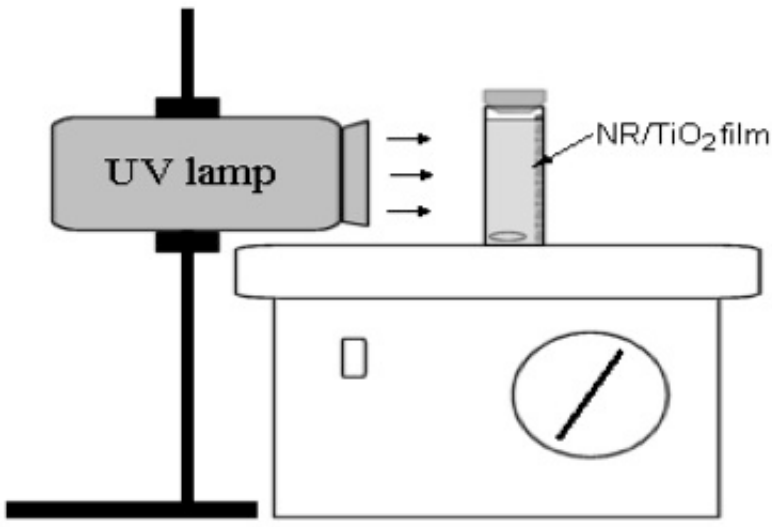

Figure 1. Schematic diagram of set up used for photocatalysis study.

comprised of a quartz cuvette, a UV source was from UV land-USA mineral light lamp model UVGL-58 (0.12 A, 220 V and 50 Hz) and a magnetic stirrer with the sample solution sealed during the photocatalysis reaction. The set up was placed in a dark Faraday Box during the test to prevent any interference from other light sources. UV light with a wavelength of 365 nm was used throughout the photocatalysis study.

RESULTS AND DISCUSSION

1-D Sodium Titanate Nanoparticles

Figure 2 shows well defined and discrete 1D nanorods with diameter in the range of 50 – 200 nm and several micrometers in length. The X-ray diffraction (XRD) patterns represent XRD information obtained from the database. All peaks can be indexed based on sodium trititanate ($Na_2Ti_3O_7$, JCPDS 00-31-1329) except the features with 2θ values at 11.5º and 36.5º. The peaks at 2θ= 10.5º, 16.0º, 25.0º, 30.0º, 34.5º, 38.0º, 44.0º, 48.5º and 53º represent the lattice planes 001, 101, 011, 300, 203, 310, 401, 020 and 413 respectively. The two absent peaks in the $Na_2Ti_3O_7$ database can be indexed to $Na_2Ti_7O_{15}$ as deposited by Wadsley in the Inorganic Crystal Structure Database (ICSD) where 2θ = 11.5º and 36.5º are corresponding to lattice planes 200 and 601 respectively. It is noted that Wang[23] obtained a similar XRD pattern but the peak at 36.5º was indexed to the 103 lattice plane of $Na_2Ti_3O_7$ due to the slightly lower 2θ position (35.5º – 36.0º) and the absence of a peak at 11.5º. A mixed phase system has also been reported by Kolen'ko[24] where three titanates with the chemical formula $Na_2Ti_nO_{n+1}$ (n = 3, 4, 9) were identified in a product of a single hydrothermal reaction. In this case, $Na_2Ti_3O_7$ and $Na_2Ti_7O_{15}$ were obtained in a single hydrothermal reaction.

Figure 3 shows the XRD pattern for the nanotubes obtained. The stick patterns are $H_2Ti_2O_5{\cdot}H_2O$ (JCPDS 00-047-0124) and $H_2Ti_3O_7$ deposited by Gateshki[25] in the ICSD. The 6 peaks found at 2θ = 10º, 24º, 28º, 39º, 48º and 63º can be indexed to lattice planes 200, 110, 310, 501, 020 and 202 respectively of hydrogen titanate, $H_2Ti_2O_5{\cdot}H_2O$. A similar XRD pattern has been reported as $H_2Ti_3O_7$ or $(Na,H)_2Ti_3O_7$ by Gateshki[25] and Suzuki[26]. This

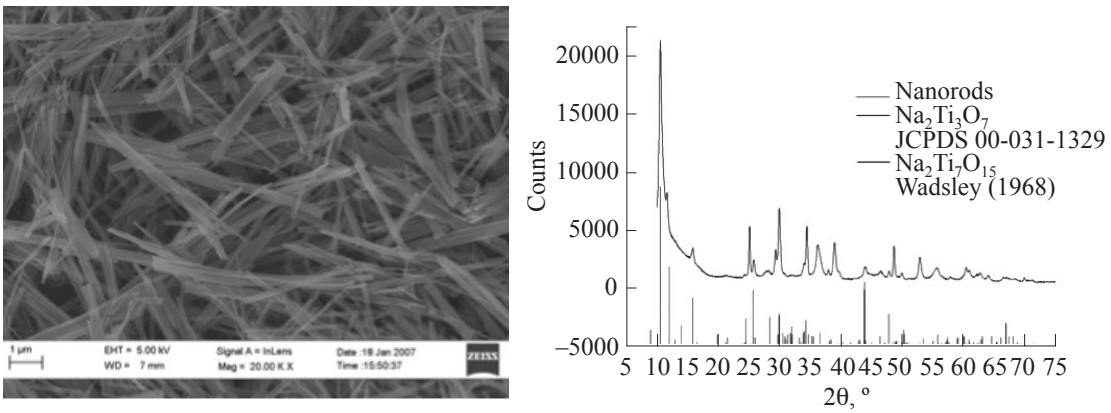

Figure 2. SEM image of 1-D sodium titanate nanorods and the corresponding XRD analysis.

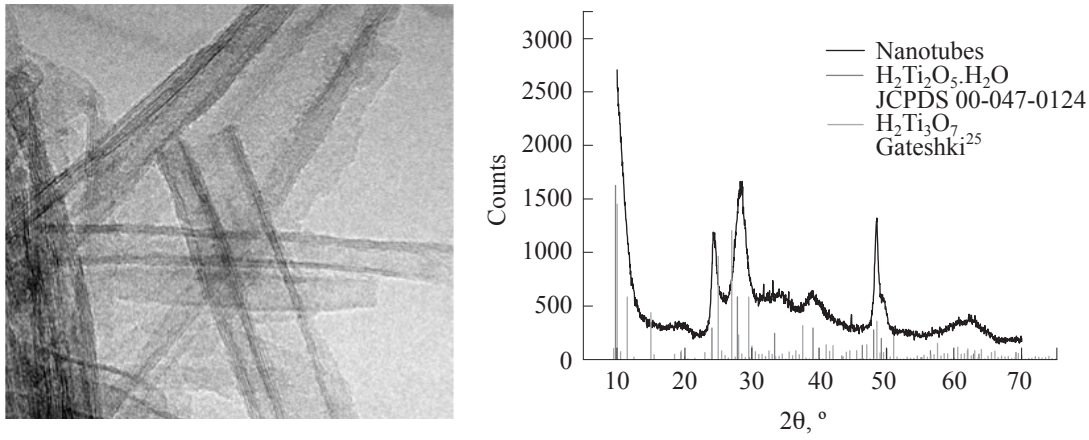

Figure 3. TEM image of 1-D sodium titanate nanotubes and the corresponding XRD analysis. The scale bar is 10 nm.

is due to very similar XRD patterns among the titanates mentioned where Na^+ can be readily replaced by H+ *via* ion exchange method. However, a peak at 2θ = 15º which belongs to $H_2Ti_3O_7$, does not appear in the nanotubes prepared in this study. In this preparation, $H_2Ti_2O_5 \cdot H_2O$ was obtained.

Rhodamine B Stability Under UV Irradiation

Rhodamine is a commonly used dye compound. Its ability of luminescence has resulted in the use as a tracer dye in water flow technology. It is also extensively used in modern biotechnology. When excited, the molecules fluorescened and the emission can be easily detected or monitored by a fluoremeter. Rhodamine B ($C_{28}H_{31}ClN_2O_3$) is a family member of rhodamine.

Rhodamine B's stability was tested under 365 nm UV light for up to four hours exposure. The test is important as a reference to ensure that the changes in emission with the presence of photocatalyst in the solution could only be due to the degradation caused by photocatalytic reaction instead of destruction due to UV irradiation. In a sample containing only rhodamine B solution, the fluorescent activity was monitored using the fluorescence peak for excitation at 510 nm as mentioned by Du[27]. *Figure 4* shows the fluorescence emission in the range 565 and 700 nm at different UV illumination times. The retention of fluorescence activity was as high as 95% after four hours of irradiation indicating that rhodamine B molecules survived intense UV illumination.

Degradation of Rhodamine B by NR/ Titanate Nanocomposite

The photocatalytic degradation pathway for rhodamine B has been studied by Chen[6], Qu[15] and He[10,28]. In brief, the decomposition of rhodamine B occurs by deethylation, followed by the destruction of chromophore. Similarly, Liu[29] concluded that the conjugated chromophore in dye molecules is destroyed at the later stage of irradiation. He also provides evidence of the presence of hydrogen peroxide

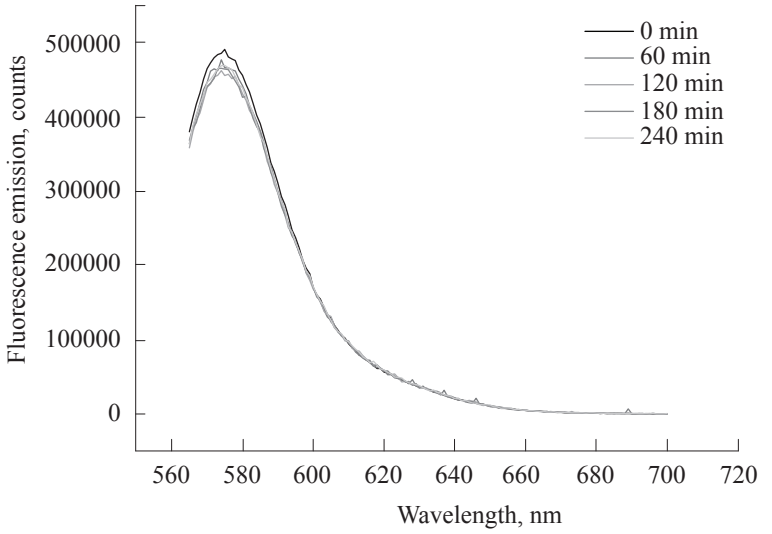

Figure 4. Rhodamine B stability test showing that in room condition rhodamine B is stable under the irradiation of UV light with 365nm wavelength. UV lamp power 26.4W.

molecules which are believed to contribute to the ring opening reaction of the conjugated chromophore. The H_2O_2 molecules are formed through the combination of hydroxyl radicals generated by photocatalysis reaction as shown in *Equation 1*:

$$OH\cdot + OH\cdot \rightarrow H_2O_2 \quad \ldots 1$$

SEM Images of NR/Titanates Nanocomposite

Figure 5 shows the SEM images of NR/titanates nanocomposites. The nanorods are clearly well distributed throughout the entire surface. However, the nanotubes are agglomerated (*Figure 6*). To enable SEM imaging, the sample of latex obtained in the SEM study was mixed with the nanoparticles and the layer of nanocomposite was drop casted on an aluminium stub rather than NR strip and dried in the oven. As the application technique was the same, the surface characteristic is assumed to be the same. If NR strip was used, heavy surface charging during SEM imaging occurred since NR is an excellent insulator and as a consequence, clear SEM images could not be obtained. However, the difference in surface properties for both aluminium and NR could have some minor effects on the coating behaviour.

Photocatalytic Activity of NR/Titanates Nanocomposite

Figure 7 shows the results of the photocatalytic study using both nanocomposite samples described earlier. The study shows that the nanoparticles embedded NR nanocomposite possesses photocatalytic activity even though at a less powerful level. The intensity of fluorescence from RhB was reduced significantly for the nanocomposite which uses smaller nanoparticles; the intensity of RhB fluorescence emission was declining steadily until no emission peak was observed

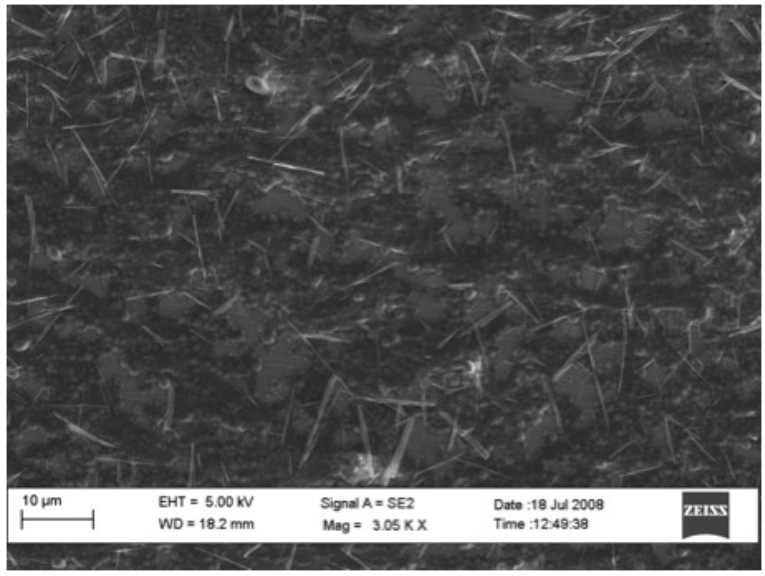

Figure 5. SEM images of NR/nanorods nanocomposite.

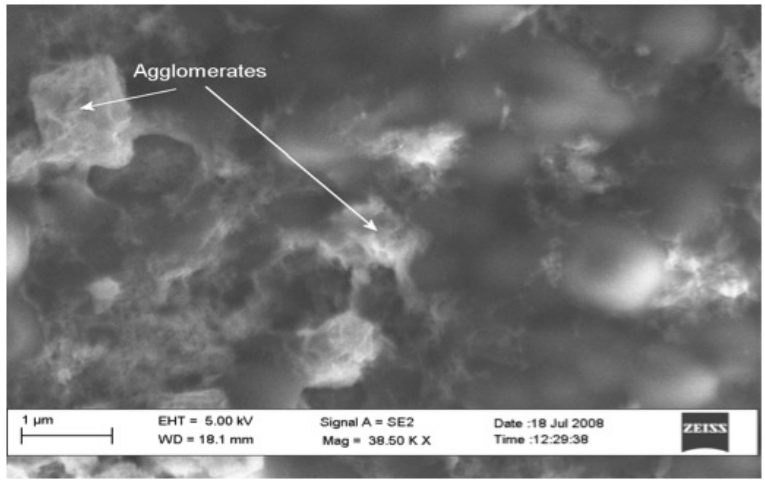

Figure 6. SEM images of NR/nanotubes nanocomposite.

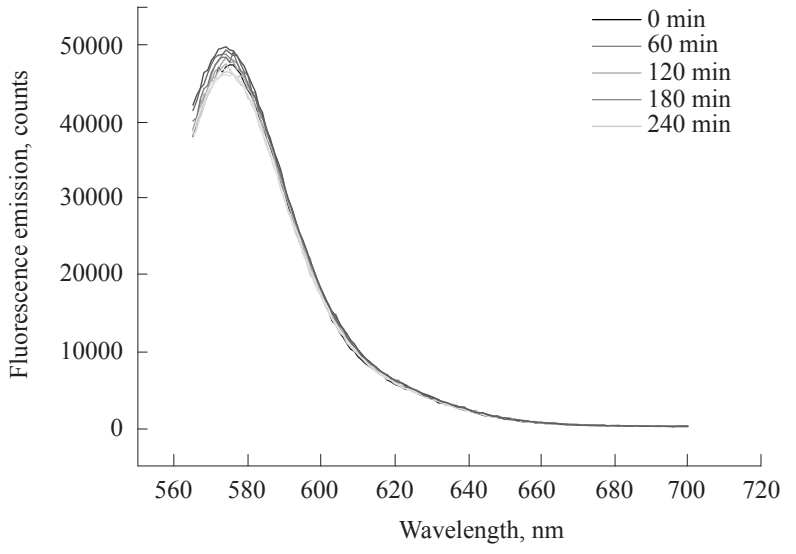

(a)

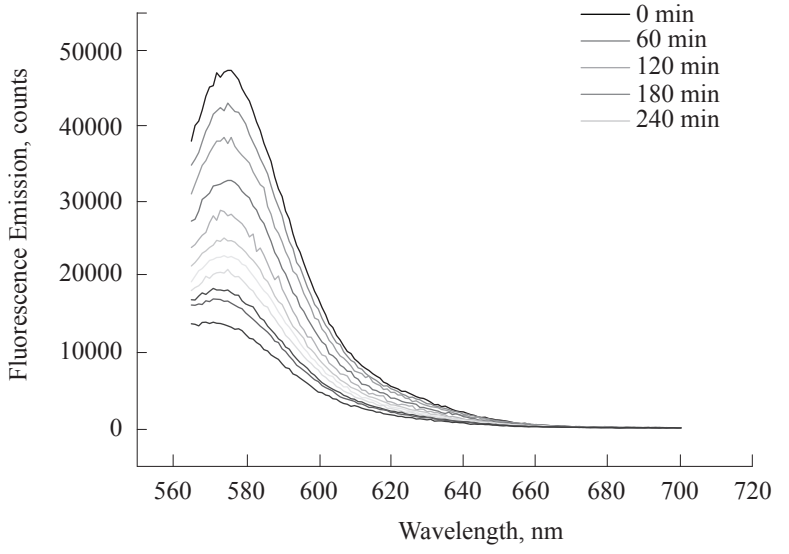

(b)

Figure 7. Schematic plots of fluorescent emission of RhB solution treated with NR/titanate nanocomposites under UV irradiation. (a) NR/nanorod and (b) NR/nanotube

after 10 hours of UV irradiation as illustrated in *Figure 8*. Given the fact that the two titanate samples are indeed different materials (based on the XRD results), differences in photoactivity should be expected. Nevertheless, the nanocomposite made of nanorods suffers photocatalytic inefficiency due to limited exposed surface area. This can be explained by the much lower exposed area of the nanorods if compared to the nanotubes. More nanotubes are seen on the surface.

An approximate calculation of the effective area of exposure was obtained by measuring the area fraction of nanoparticles in an SEM image. It is noted that the measurement is just an approximation because there are areas where the particles appear to be seen but not clear, indicating a thin layer of coating material covering the particles. As the effectiveness of these particles is uncertain, the accurate surface area that is exposed to the RhB solution is difficult to be measured accurately. The area fraction for nanorods on the surface of the nanocomposite as seen in the SEM image in *Figure 5* is approximately 7.1%. From the area fraction values, it is possible to work out the number of nanoparticles found on the entire nanocomposite surface. It is calculated that the number of nanorods estimated on the nanocomposite surface is around 2% of the total nanorods loaded. This is an indication that most of the nanorods were buried by the NR particles. Due to the significant density difference between titania and NR, sedimentation can occur during the drying process. The area for nanotubes containing nanocomposite as shown in *Figure 6* is approximately 40%. It was noted that the distribution of nanotubes on the nanocomposite surface was not homogeneous and some agglomerates were found. In this

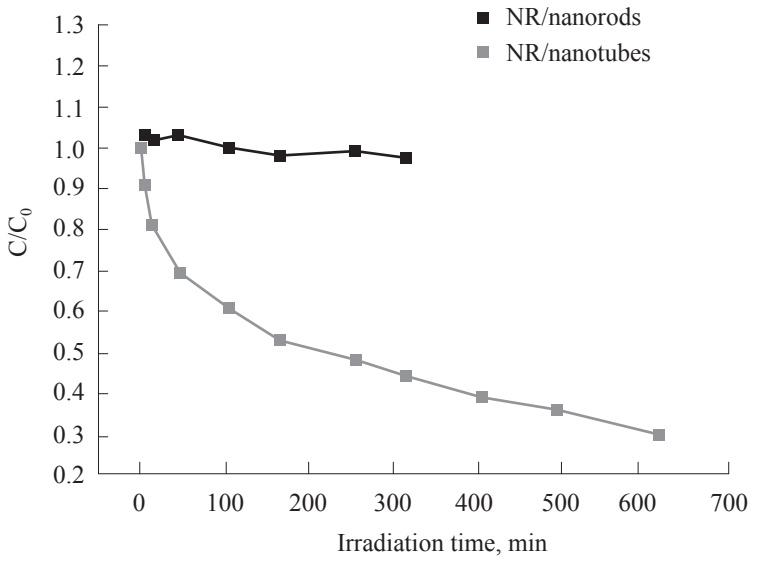

Figure 8. Schematic plot showing that only the NR/nanotubes sample is photocatalytically active and capable of reducing RhB's fluorescent emission intensity down to less than 30% of its original value after 10 hours of UV irradiation.

case the number of nanotubes cannot be obtained using the same approach as for nanorods. This is due to the orientation of the nanotubes on the nanocomposite surface and the agglomeration of nanotubes. However, it is expected that the number of nanotubes on the nanocomposite surface is higher due to the lower specific density. Furthermore, the surface area of a nanotube is much higher than that of a nanorod, as mentioned earlier, further enhancing activity.

In order for the degradation of RhB molecules to happen, adsorption of RhB molecules to the catalysts must occur. The quantity of adsorption is substantially lower for NR/nanorods nanocomposite because the nanoparticles are embedded into the NR matrix. The immobilised nanoparticles therefore have less effective surface area for the absorption process. As a result, this NR/nanorod nanocomposite was classified as photocatalytically inactive. The number density of nanoparticles can be increased to improve the reaction rate but that could bring adverse effects to the nanocomposite such as increased particle counts and potentially affect the flexibility or elasticity of the NR surface.

CONCLUSION

The XRD results show that the nanorods and nanotubes obtained were mixed phase sodium trititanate ($Na_2Ti_3O_7$ and $Na_2Ti_7O_{15}$) and hydrogen titanate ($H_2Ti_2O_5 \cdot H_2O$) respectively. It can be concluded that the well defined 1-D titanates nanoparticles synthesised in this study are photocatalytically active. The type of particles plays an important role in the rate of photocatalysis, as shown by the degradation rate of rhodamine B under UV irradiation. Being different in the crystal structure, the photocatalytic activity of nanorods and nanotubes is expected to be different. The ineffectiveness of NR/nanorods naocomposite is probably due to the limited exposed area of nanorods as seen in SEM images.

Date of receipt: October 2010
Date of acceptance: March 2011

REFERENCES

1. SUNADA, K., KIKUCHI, Y., HASHIMOTO, K. AND FUJISHIMA, A. (1998) Bactericidal and Detoxification Effects of TiO2 Thin Film Photocatalysts. *Environ. Sci. Technol*., **32(5)**, 726–728.

2. SUNADA, K., WATANABE, T. AND HASHIMOTO, K. (2003) Studies on Photokilling of Bacteria on TiO2 Thin Film. *J. Photoch. Photobio. A: Chem*., **156(1-3)**, 227–233.

3. MAHLTIG, B., GUTMANN, E., MEYER, D. C., REIBOLD, M., DRESLER, B., GUNTHER, K., FASSLER, D. AND BOTTCHER, H. (2007) Solvothermal Preparation of Metallized Titania Sols for Photocatalytic and Antimicrobial Coatings, *J. Mater. Chem*., **17(22)**, 2367–2374.

4. KOIDE, S. AND NONAMI, T. (2007) Disinfecting Efficacy of a Plastic Container Covered with Photocatalyst for Postharvest. *Food Control*, **18(1)**, 1–4.

5. MA, Y. AND YAO, J. (1999) Comparison of Photodegradative Rate of Rhodamine B Assisted by Two Kinds of TiO2 Films. *Chemosphere*, **38(10)**, 2407–2414.

6. CHEN, F., ZHAO, J. C. AND HIDAKA, H. (2003) Highly Selective Deethylation of Rhodamine B: Adsorption and Photooxidation Pathways of the Dye on the TiO2/SiO2 Composite Photocatalyst. *Inter. J. Photoenergy*, **5(4)**, 209–217.

7. WILHELM, P. AND STEPHAN, D. (2007) Photodegradation of Rhodamine B in Aqueous Solution Via SiO2@TiO2 Nano-

Spheres. *J. Photoch. Photobio. A: Chem*. **185(1)**, 19–25.

8. LI, J., MA, W., LEI, P. AND ZHAO, J. (2007) Detection of Intermediates in the TiO2-Assisted Photodegradation of Rhodamine B Under Visible Light Irradiation. *J. Environ. Sci*., **19(7)**, 892–896.

9. LI, J., LIU, L., SIQIN, G. AND BAI, T. (2007) Study of the Photocatalytic Degradation of Rhodamine B on TiO2/clinoptilolite. *Ganguang Kexue yu Guanghuaxue/ Photographic Sci. Photochem*., **25(4)**, 284–295.

10. HE, Z., YANG, S., JU, Y. AND SUN, C. (2009) Microwave Photocatalytic Degradation of Rhodamine B using TiO2 Supported on Activated Carbon: Mechanism Implication, *J. Environ. Sci*., **21(2)**, 268–272.

11. BELVER, C., ADAN, C., AND FERNDEZ-GARC, M. Photocatalytic Behaviour of Bi2MO6 Polymetalates for Rhodamine B Degradation. *Catalysis Today*. In Press, Corrected Proof.

12. WAHI, R.K., YU, W. W., LIU, Y., MEJIA, M.L., FALKNER, J.C., NOLTE, W. AND COLVIN, V.L. (2005) Photodegradation of Congo Red Catalyzed by Nanosized TiO2. *J. Mol. Catalysis A: Chem*., **242(1-2)**, 48–56.

13. TERATANI, S., NAKAMICHI, J., TAYA, K. AND TANAKA, K. (1982) Photocatalytic Dehydrogenation of 2-Propanol Over TiO2 and Metal TiO2 Powders. *Bull. Chem. Soc. Japan*, **55(6)**, 1688–1690.

14. ANPO, M., YAMASHITA, H., ICHIHASHI, Y., FUJII, Y., AND HONDA, M. (1997) Photocatalytic Reduction of CO_2 with H_2O on Titanium Oxides Anchored within Micropores of Zeolites: Effects of the Structure of the Active Sites and the Addition of Pt. **101(14)**, *J. Phys. Chem. B*, 2632–2636.

15. QU, P., ZHAO, J., SHEN, T. AND HIDAKA, H. (1998) TiO2-Assisted Photodegradation of Dyes: A Study of Two Competitive Primary Processes in the Degradation of RB in an Aqueous TiO2 Colloidal Solution. *J. Mol. Catalysis A: Chem*., **129(2-3)**, 257–268.

16. ZHAO, Y., LI, C., LIU, X. AND GU, F. (2007) Highly Enhanced Degradation of Dye with Well-Dispersed TiO2 Nanoparticles Under Visible Irradiation. *J. Alloys Compounds*, **440(1-2)**, 281–286.

17. WANG, Y.W., ZHANG, L.Z., DENG, K.J., CHEN, X.Y. AND ZOU, Z.G. (2007) Low Temperature Synthesis and Photocatalytic Activity of Rutile TiO2 Nanorod Superstructures. *J. Phys. Chem. C*., **111(6)**, 2709–2714.

18. LI, J.Y., MA, W.H., CHEN, C.C., ZHAO, J.C., ZHU, H.Y. AND GAO, X.P. (2007) Photodegradation of Dye Pollutants on One-Dimensional TiO2 Nanoparticles Under UV and Visible Irradiation. *J. Mol. Catalysis a-Chemical*, **261(1)**, 131–138.

19. SONG, X., WU, J. AND YAN, M. Photocatalytic Degradation of Selected Dyes by Titania Thin Films with various Nanostructures. *Thin Solid Films*. In Press, Accepted Manuscript.

20. SRIWONG, C., WONGNAWA, S. AND PATARAPAIBOOLCHAI, O. (2008) Photocatalytic Activity of Rubber Sheet Impregnated with TiO2 Particles and its Recyclability. *Catalysis Communications*. **9(2)**, 213–218.

21. GAO, Y. AND LIU, H. (2005) Preparation and Catalytic Property Study of a Novel Kind of Suspended Photocatalyst of TiO2-Activated Carbon Immobilized on Silicone Rubber Film. *Mater. Chem. Physics*, **92(2-3)**, 604–608.

22. NAWI, M.A., KEAN, L.C., TANAKA, K. AND JAB, M.S. (2003) Fabrication of Photocatalytic TiO2-Epoxidised Natural Rubber on Al Plate Via Electrophoretic Deposition. *Applied Catalysis B: Environmental*, **46(1)**, 165–174.

23. WANG, L., ZHANG, T., QI, Q., HU, J., ZENG, Y. AND LU, G. (2009) Synthesis and Field Effect Characteristics of $Na_2Ti_3O_7$ Nanowires. *Mater. Lett.*, **63(11)**, 903–904.

24. KOLEN'KO, Y.V., KOVNIR, K.A., GAVRILOV, A.I., GARSHEV, A.V., FRANTTI, J., LEBEDEV, O.I., CHURAGULOV, B.R., VAN TENDELOO, G. AND YOSHIMURA, M. (2006) Hydrothermal Synthesis and Characterization of Nanorods of Various Titanates and Titanium Dioxide. *J. Phys.Chem. B*. 1104030-4038.

25. GATESHKI, M., CHEN, Q., PENG, L., CHUPAS, P. AND PETKOV, V. (2007) Structure of Nanosized Materials by High-Energy X-Ray Diffraction: Study of Titanate Nanotubes. *apo. ansto.,* 222612–616.

26. SUZUKI, Y. AND YOSHIKAWA, S. (2004) Synthesis and Thermal Analyses of TiO2-Derived Nanotubes Prepared by the Hydrothermal Method. *J. Mater. Res*., **19(4)**, 982–985.

27. DU, H., FUH, R.-. A., LI, J., CORKAN, L.A. AND LINDSEY, J.S. (1998) PhotochemCAD?: A Computer-Aided Design and Research Tool in Photochemistry. J. *Photoch. Photobio*., **68(2)**, 141–142.

28. HE, Z., SUN, C., YANG, S., DING, Y., HE, H. AND WANG, Z. (2009) Photocatalytic Degradation of Rhodamine B by $Bi_2WO_6$with Electron Accepting Agent Under Microwave Irradiation: Mechanism and Pathway. *J. Hazard. Mater.*, **162(2-3)**, 1477–1486.

29. LIU, G.M. AND ZHAO, J. (2002) TiO2-Photosensitized Decomposition of Dye Pollutant Sulforhodamine B Under Visible Light Irradiation. *J. Adv. Oxid. Technol.*, **5(1)**, 72–76.